The Emerald Research Register for this journal is available at
www.emeraldinsight.com/researchregister

The current issue and full text archive of this journal is available at
www.emeraldinsight.com/0961-5539.htm

Received January 2002
Revised July 2003
Accepted September 2003

The two-fluid modelling of gas-particle transport phenomenon in confined systems considering inter particle collision effects

A. Mitter
CMERI, Durgapur, West Bengal, India
J.P. Malhotra
Aerospace Engineering Department IIT, Kharagpur, West Bengal, India
H.T. Jadeja
CMERI, Durgapur, West Bengal, India

Keywords *Flow, Turbulence, Gases*

Abstract *A modelling approach of gas solid flow, considering different physical phenomenon such as fluid turbulence, particle turbulence and interparticle collision effects are presented. The approach is based on the two-fluid model formulation where both phases are treated as continuum. This implies that the gas phase as well as the particle phase are weighted by their separate volumetric fractions. According to the experimental results and numerical simulations, the inter-particle collision possesses a significant influence of turbulence level on particle transport properties in gas solid turbulent flow even for dispersed phase volume fraction ($\alpha < 0.01$). Comparisons in predictions have been depicted with inclusion of interparticle collision effect in the equation of particle turbulent kinetic energy and with exclusion of this effect. Experimental research has been conducted in a thermal power plant depicting higher erosion resistance of noncircular square sectioned coal pipe bends in comparison with those with circular cross section, the salient features of the experimental work are presented in this paper. Experiments have been conducted to determine, pressure drop in straight and curved portions of conduits conveying air coal mixtures in a thermal power plant. Validation of this experimental data with numerical predictions have been presented.*

The authors are extremely grateful to Professor B.N. Sreedhar, Aerospace Engineering Department, IIT Kharagpur and Dr K.M. Kundu, Deputy Director, CMERI for their valuable advice and suggestions on the research work carried out. The authors express their deep and innermost gratitude to Professors O. Simonin, Clive Fletcher, Jiyuan Tu, Lixing Zhou and F. Durst for their pioneering research on turbulent two phase flow and sending some of their valuable publications. The authors express their deep regards and gratefulness to Professor D.B. Spalding for his encouragement, also dissemination of fundamental knowledge on CFD and general turbulence models. The authors finally express their sincere and innermost gratitude to Professor K.N. Seetharamu for his constant inspiration in this research and Director CMERI for his kind support.

International Journal of Numerical Methods for Heat & Fluid Flow
Vol. 14 No. 5, 2004
pp. 579-605

0961-5539
DOI 10.1108/09615530410539937

Nomenclature

C_D = drag coefficient
d_p = particle diameter
D_e = dean number
F_{WM} = wall momemtum exchange term due to particle wall collision
f = correction factor to Stoke's drag coefficient
g = acceleration due to gravity
H = distance along height from bottom wall to axisymmetric plane of square duct
K, k = turbulence kinetic energy
K_p, k_p = particle turbulence kinetic energy
K_{gp}, k_{gp} = gas particle covariance
m = particle mass loading ratio
P = pressure in cross stream plane
p = mean pressure in longitudinal direction
R = radius of circular duct
R_{ep} = particle Reynolds number
S_{ui} = fluid particle interaction term (drag force) in fluid phase equation gravitational term and additional source term due to curvature in curved passage $-\beta\rho g \; -0.75\alpha\beta\frac{C_D\mu}{d_p^2}R_{ep}(u_i - u_{pi})$
S_{pi} = fluid particle interaction term (drag force) in particle phase equation and gravitational term $-\alpha\rho_p g + 0.75\alpha\beta\frac{C_D\mu}{d_p^2}R_{ep}(u_i - u_{pi})$
u_i, u_j = fluid velocities in the ith and jth directions, respectively
u_{pi}, u_{pj} = particle velocities in the ith and jth directions, respectively
WIDTH = width of the channel (rectangular) or circumference of a semicircle
X = distance along the width of a channel
Y = distance along the height of a square channel or radial distance for a circular channel from center, i.e. $y = 0$ at center
Y_1 = radial distance from wall of a circular duct, $Y_1 = 0$ at wall
ρ = fluid density
ρ_p = particle density
α = particle concentration or particle volume fraction
β = volume fraction of the gas
ε = dissipation rate of turbulence
μ = fluid viscosity
μ_{eff} = effective viscosity of fluid phase
μ_{efp} = effective viscosity of particle phase

Subscript

Cl = center line of duct
l = laminar
max = maximum

Introduction

The two phase gas particle flows have wide industrial application in chemical process plants, thermal power engineering, etc. The pressure drop characteristics in two phase turbulent transport is very important for design of conduits conveying two phase gas-solid mixture. In practical situation where particles are abrasive in nature, serious erosive wear may occur in pipelines conveying gas-particle flows, e.g. coal pipe bend sections in thermal power plants conveying air-coal mixtures. (Tsirkunov *et al.* 2002) adopted Lagrangian approach for numerical treatment of the dispersed phase in dilute two phase flows. Sommerfeld (2001, 2003) introduced interparticle and wall particle collision effects in the frame of Lagrangian approach for the particle phase.

The paper aims at predictions of turbulent two phase gas particle flows based on the Eulerian approach. In the two-fluid model, the two phases are treated as two separate interpenetrating continua and mean equations are solved for both phases and coupled through interphase mass and momentum transfer terms. Gidaspow (1994) provides a kinetic theory interpretation of the continuum approach for dispersed phase. Mitter *et al.* (1993, 1998) have presented a crude two-fluid model in which wall particle collision effects and fluid turbulence modulation effects were not considered. The particle phase eddy viscosity was expressed in terms of fluid phase eddy viscosity through an algebraic relation presented by Choi and Chung (1983). Tu and Fletcher (1995) have also utilised a similar algebraic relation between dispersed phase eddy viscosity and carrier phase eddy viscosity for analysing two phase flow fields in curved duct. Zhang and Reese (2001) introduced particle gas turbulence interactions in a kinetic theory approach to granular flow. This kinetic theory has been detailed by Gidaspow (1994). The present approach considers fluid turbulence modulation effects due to the presence of particles and wall particle collision effects to generate suitable Eulerian boundary conditions of the dispersed phase. A particulate turbulence model based on separate transport equations for the dispersed phase turbulent kinetic energy and fluid particle covariance consisting of interphase transfer terms has been employed for modelling the dispersed phase turbulent viscosity. Hence, the K-ε-K_p-K_{gp} model is utilised.

The interparticle collision effects are found to have influence on dilute two phase transport phenomenon at turbulence level resulting in return to isotropy contribution in particle kinetic stress transport equations. This feature has been depicted by He and Simonin (1993) and Simonin (1996). The resulting model is based on Grad's kinetic theory of dilute gases. The extension of Grad's theory to inelastic particles leads to a complementary dissipative term in the particle kinetic stress transport equation. This aspect has also been considered in present predictions. The numerical predictions of three dimensional turbulent two phase flow fields have been depicted. Comparison has been shown between the predictions based on K_p equation including interparticle collision effect and excluding this effect.

The numerical predictions are compared with the experimental data of Tanaka *et al.* presented by He and Simonin (1993) for vertical straight pipes to validate the present computations. The computations are also extended to curved ducts of noncircular cross section. The predicted effects of Dean number and particle size on particle concentration profile are presented. The coal pipe bends of circular section are subjected to serious erosion owing to localised particle concentration on the outer wall. This feature has been shown through numerical predictions of the particle concentration profile. The experimental research was based upon design modification of a coal pipe bend to reduce erosion. The comparison of erosion data for this design with that of a conventional design under operational conditions has been depicted. The pressure drop measurements on two phase flow of air coal mixtures in straight and curved portions of coal pipes are compare well with the numerical computations and the results are shown in this paper.

Mathematical formulation for two phase turbulent transport using Eulerian approach

The mathematical modelling based on the two fluid approach considers both fluid phase and dispersed phase as two interpenetrating continua which exchange mass, momentum and energy with each other. The strong analogy between the random motion of particles in turbulent flow and thermal motion of gas molecules leads to the application of kinetic theory approach to derive the continuum equations for the particle phase. The two-fluid model approach has been adopted by Durst and Milojevic (1984), He and Simonin (1993), Rizk and Elghobashi (1989), Simonin (1996) and Tu and Fletcher (1996) for the range of particle volumetric fraction considered in this paper, i.e. $\alpha = 3\times10^{-4}$-5.13×10^{-3}.

In dilute two-phase flows, the continuum modelling of the dispersed phase fluctuating motion was achieved by several authors using the algebraic models obtained in the framework of Tehen's theory of discrete particles suspended in homogeneous fluid turbulence. This approach was validated by comparison of numerical predictions with various experimental data. However, due to the assumption of local particle entrainment by the surrounding fluid turbulence, these models cannot account for important physical mechanism governing the turbulent velocity correlations and particle dispersion in gas solid flows, such as shearing of the dispersed phase flow, interparticle and particle-wall collisions. Hence, the next section deals with modified Eulerian modelling of the two phase flow field.

The following mathematical models representing the fluid and particle phase are for a straight rectangular duct. Generalised Eulerian solid surface boundary conditions for the particulate phase are employed through particle-wall collision effect (Tu *et al.*, 1996). In the momentum balance equation the particulate phase momentum exchanges with solid walls are included. The turbulence closure for the gas phase is effected by using the RNG based K-ε model (Tu and Fletcher, 1995, 1996). An exponential form of the additional source terms in K and ε equations for turbulence modulation suggested by Tu and Fletcher (1994) has also been utilised. The separate transport equations for particle turbulent kinetic energy K_{p} and gas particle covariance K_{gp} consisting of interphase transfer terms are being solved to generate the particle phase eddy viscosity as described by Mitter (2000), Tu (1997), Tu and Fletcher (1996) and Zhou *et al.* (1994). The equations for K_{p} and K_{gp} are derived from Favre averaged conservation equations for both gas and particulate phases, and the equations have been modelled based on physical analysis. These transport models provide adequate description of anisotropy of the particle velocity fluctuations. For curved ducts and pipes of circular cross sections, etc., various additional source terms are included in the momentum equations. These terms include additional viscous sources, centrifugal acceleration, etc. The validation of the turbulence model and closure assumption have been carried out in comparison with the present numerical predictions and various computations and experimental data based on Laser Doppler Velocimeter measurement.

Equations for the fluid phase

Equation of continuity

$$\frac{\partial}{\partial x_j}(\beta \rho u_j) = 0 \tag{1}$$

where $\beta = 1 - \alpha$

Equation of momentum

$$\frac{\partial}{\partial x_j}(\beta \rho u_i u_j) = -\beta \frac{\partial p}{\partial x_i} + \frac{\partial}{\partial x_j}\left\{\beta \mu_{\mathrm{eff}}\left(\frac{\partial u_i}{\partial x_j} + \frac{\partial u_j}{\partial x_i}\right)\right\} + S_{\mathrm{u}i} \tag{2}$$

Turbulence kinetic energy

$$\frac{\partial}{\partial x_j}(\beta \rho u_j k) = \frac{\partial}{\partial x_j}\left\{\left(\frac{\beta u_{\mathrm{eff}}}{\sigma_\kappa}\frac{\partial k}{\partial x_j}\right)\right\} + \beta G - \beta \rho \varepsilon + S_k \tag{3}$$

where

$$G = \mu_{\mathrm{eff}}\left(\frac{\partial u_i}{\partial x_j} + \frac{\partial u_j}{\partial x_i}\right)\frac{\partial u_i}{\partial x_j}$$

Dissipation rate

$$\frac{\partial}{\partial x_j}(\beta \rho u_j \varepsilon) = \frac{\partial}{\partial x_j}\left\{\left(\frac{\beta u_{\mathrm{eff}}}{\sigma_\varepsilon}\frac{\partial \varepsilon}{\partial x_j}\right)\right\} + \frac{\beta C_1 \varepsilon G}{k} - \frac{\beta C_2 \rho \varepsilon^2}{k} + S_\varepsilon - \beta \rho R \tag{4}$$

$$\mu_{\mathrm{eff}} = \mu_1 + \frac{C_\mu \rho k^2}{\varepsilon}$$

The rate of strain term R in the ε equation is expressed as:

$$R = \frac{C_\mu \eta^3 (1 - \eta/\eta_0)\varepsilon^2}{(1 + \beta_0 \eta^3)k} \tag{5}$$

and

$$\eta = \frac{k}{\varepsilon}\left(2S_{ij}^2\right)^{\frac{1}{2}}, \quad S_{ij} = \frac{1}{2}\left(\frac{\delta u_i}{\delta x_j} + \frac{\delta u_j}{\delta x_i}\right)$$

where $\beta_0 = 0.0015$ and $\eta_0 = 4.38$

According to RNG theory the constants in the turbulent transport equations are:

$$C_\mu = 0.0845, \quad C_1 = 1.42, \quad C_2 = 1.68, \quad \sigma_k = 1.0, \quad \sigma_\varepsilon = 1.3$$

For the confined two-phase flows, the effect of the particulate phase on the turbulence structure of the gas phase are modelled as:

$$S_k = -\frac{2f}{t_\mathrm{p}}\alpha\rho_\mathrm{p}(k - k_\mathrm{gp}) \tag{6a}$$

in the k-equation and

$$S_\varepsilon = -\frac{2f}{t_\mathrm{p}}\alpha\rho_\mathrm{p}(\varepsilon - \varepsilon_\mathrm{gp}) \tag{7a}$$

in the ε-equation, where f is the correction factor to Stoke's drag coefficient and t_p is the particle relaxation time.

Tu and Fletcher (1994) suggest the following forms for modelling the additional dissipation terms S_κ and S_ε in the K- and ε-equation, respectively.

$$S_\kappa = -2k\left(\frac{\alpha\rho_\mathrm{p}}{t_\mathrm{p}}\right)\left\{1 - \exp\left(-\frac{B_k t_\mathrm{p}}{t_\mathrm{L}}\right)\right\} \tag{6b}$$

and

$$S_\varepsilon = -2\varepsilon\left(\frac{\alpha\rho_\mathrm{p}}{t_\mathrm{p}}\right)\left\{1 - \exp\left(-\frac{B_\varepsilon t_\mathrm{p}}{t_\mathrm{L}}\right)\right\} \tag{7b}$$

where B_K and B_ε are the empirical constants provided in Tu and Fletcher (1994, 1996) and t_L is the Lagrangian integral time scale.

For computation of turbulent flows in near wall regions the wall function method outlined by Patankar *et al.* (1975) has been adopted owing to its economy from points of view of computer storage and time. Hence, it is assumed that a logarithmic velocity profile prevails in the region between wall and near wall node.

Equation for particle phase

Equation of continuity

$$\frac{\partial}{\partial x_j}(\alpha \rho_{\mathrm{p}} u_{\mathrm{p}j}) = 0 \tag{8}$$

Equation of momentum

$$\frac{\partial}{\partial x_j}(\alpha \rho_{\mathrm{p}} u_{\mathrm{p}i} u_{\mathrm{p}j}) = -\frac{\alpha\, \partial p}{\partial x_i} + \frac{\partial}{\partial x_j}\left\{\alpha \mu_{\mathrm{efp}}\left(\frac{\partial u_{\mathrm{p}i}}{\partial x_j} + \frac{\partial u_{\mathrm{p}j}}{\partial x_i}\right)\right\} + S_{\mathrm{p}i} + F_{\mathrm{WM}} \tag{9}$$

The terms $S_{\mathrm{u}i}$ in equation (2) and $S_{\mathrm{p}i}$ in equation (9) are defined in the nomenclature.

Let ε_{f} and ε_{p} be the kinematic eddy viscosity of the gas and particle phases, respectively. The transport equations governing the particulate turbulent kinetic energy and gas particle covariance are given as follows.

Particle turbulent kinetic energy equation

$$\frac{\partial}{\partial x_j}(\alpha \rho_{\mathrm{p}} u_{\mathrm{p}j} k_{\mathrm{p}}) = \frac{\partial}{\partial x_j}\left(\alpha \rho_{\mathrm{p}} \frac{\varepsilon_{\mathrm{p}}}{\sigma_{\mathrm{p}}} \frac{\partial k_{\mathrm{p}}}{\partial x_j}\right) + P_{\mathrm{kp}} - I_{\mathrm{gp}} \tag{10}$$

where the turbulence production of the particle phase is:

$$P_{\mathrm{kp}} = \alpha \rho_{\mathrm{p}} \varepsilon_{\mathrm{p}}\left(\frac{\delta u_{\mathrm{p}i}}{\delta x_j} + \frac{\delta u_{\mathrm{p}j}}{\delta x_i}\right)\frac{\delta u_{\mathrm{p}i}}{\delta x_j} - \frac{2}{3}\alpha \rho_{\mathrm{p}} \delta_{ij}\left(k_{\mathrm{p}} + \varepsilon_{\mathrm{p}} \frac{\delta u_{\mathrm{pm}}}{\delta x_{\mathrm{m}}}\right)\frac{\delta u_{\mathrm{p}j}}{\delta x_j}$$

and the turbulence interaction between the two phases gives:

$$I_{\mathrm{gp}} = \frac{2f}{t_{\mathrm{p}}} \alpha \rho_{\mathrm{p}} (k_{\mathrm{p}} - k_{\mathrm{gp}})$$

where the correction factor f defined by Tu and Fletcher (1996) is selected as follows:

$$f = \begin{bmatrix} 1 + 0.15 R_{\mathrm{ep}}^{0.687} & \ldots & 0 < R_{\mathrm{ep}} \le 200 \\ 0.914 R_{\mathrm{ep}}^{0.282} + 0.0135 R_{\mathrm{ep}} & \ldots & 200 < R_{\mathrm{ep}} \le 2,500 \\ 0.0167 R_{\mathrm{ep}} & \ldots & 2,500 < R_{\mathrm{ep}} \end{bmatrix}$$

The gas-particle covariance equation

$$\frac{\partial}{\partial x_j}\{\alpha \rho_{\mathrm{p}} (u_j + u_{\mathrm{p}j}) k_{\mathrm{gp}}\} = \frac{\partial}{\partial x_j} \alpha \rho_{\mathrm{p}} \left(\frac{\varepsilon_f}{\sigma_f} + \frac{\varepsilon_{\mathrm{p}}}{\sigma_{\mathrm{p}}}\right)\frac{\partial k_{\mathrm{gp}}}{\partial x_j} + P_{\mathrm{kgp}} - \alpha \rho_{\mathrm{p}} \varepsilon_{\mathrm{gp}} - \pi_{\mathrm{gp}} \tag{11}$$

where the turbulence production by the mean velocity gradiants of two phases is:

$$P_{\mathrm{kgp}} = \frac{1}{2}\left\{ \alpha\rho_{\mathrm{p}}\left(\varepsilon_f \frac{\delta u_i}{\delta x_j} + \varepsilon_{\mathrm{p}} \frac{\delta u_{\mathrm{p}i}}{\delta x_i} \right) - \frac{2}{3}\alpha\rho_{\mathrm{p}}\delta_{ij}k_{\mathrm{gp}} \right.$$

$$\left. - \frac{1}{3}\alpha\rho_{\mathrm{p}}\delta_{ij}\left(\varepsilon_f \frac{\delta u_{\mathrm{pm}}}{\delta x_{\mathrm{m}}} + \varepsilon_{\mathrm{p}} \frac{\delta u_{\mathrm{pm}}}{\delta x_{\mathrm{m}}} \right) \right\} \left(\frac{\delta u_i}{\delta x_j} + \frac{\delta u_{\mathrm{p}i}}{\delta x_j} \right)$$

The interaction term between the two phases:

$$\pi_{\mathrm{gp}} = \frac{f}{2t_{\mathrm{p}}}\alpha\rho_{\mathrm{p}}\left[(1+m)2k_{\mathrm{gp}} - 2k - 2mk_{\mathrm{p}} \right]$$

where m is the particle mass loading.

The dissipation term due to gas viscous effect $\varepsilon_{\mathrm{gp}}$ is given by

$$\varepsilon_{\mathrm{gp}} = \varepsilon \exp(-B_\varepsilon t_{\mathrm{p}}/t_{\mathrm{L}})$$

where $t_{\mathrm{L}} = k/\varepsilon$, and $B_\varepsilon = 0.4$

The turbulent eddy viscosity of the particulate phase is defined as:

$$\varepsilon_{\mathrm{p}} = l_{\mathrm{p}\varepsilon}\sqrt{\frac{2}{3}k_{\mathrm{p}}}$$

The characteristic length $l_{\mathrm{p}\varepsilon}$ (Tu and Fletcher, 1996) of the particulate phase is modelled as:

$$l'_{\mathrm{p}\varepsilon} = \frac{l_{\mathrm{gr}}}{2}(1+\cos^2\theta)\exp\left[-B_{\mathrm{gp}}\frac{|u''_{\mathrm{r}}|}{|u''_{\mathrm{g}}|}\sin(k_{\mathrm{g}} - k_{\mathrm{p}}) \right] \tag{12}$$

where l_{gr} is the characteristic length scale of gas phase. l_{gr} is defined in terms of k and ε (Tu and Fletcher, 1996) as

$$l_{\mathrm{gr}} = \sqrt{\frac{3}{2}}\frac{C_\mu k^{3/2}}{\varepsilon},$$

In the above equation θ is the angle between the velocity of the particle and the velocity of the gas to account for the crossing trajectories effect. B_{gp} is a constant determined experimentally as $B_{\mathrm{gp}} = 0.01$. D is the characteristic length of the system.

$$l_{\mathrm{p}\varepsilon} = \min(l'_{\mathrm{p}\varepsilon}, D)$$

The relative fluctuating velocity is given by:

$$u''_{\mathrm{r}} = u''_{\mathrm{g}} - u''_{\mathrm{p}} \tag{13}$$

and

$$|u''_{\mathrm{r}}| = \sqrt{\frac{2}{3}(k_{\mathrm{g}} - 2k_{\mathrm{gp}} + k_{\mathrm{p}})} \tag{14}$$

In the above equations, the subscripts g and p refers to the gas particle phases, respectively.

Eulerian modelling of particle wall collisions via a Lagrangian approach

In order to improve the Eulerian modelling of mean particulate flow behaviour near the wall, a one dimensional model is used to derive the particle wall rebounding distance and the reflected particle velocity behaviour near the wall. The derivation has been shown by Tu *et al.* (1996). This approach has been utilised by Mitter (2000).

The particle rebounding distance is computed as follows:

$$y_{\mathrm{n}} = \frac{t_{\mathrm{p}}}{f}\left[u'_{\mathrm{p},0} - |u_{\mathrm{g}}|_{\mathrm{ref}} l_{\mathrm{n}}\left(\frac{u'_{\mathrm{p},0}}{|u_{\mathrm{g}}|_{\mathrm{ref}}} + 1\right)\right] \tag{15}$$

where $u'_{\mathrm{p},0}$ is the initial velocity of the reflected particle.

The reflected particle velocity as a function of the distance from the wall is given by:

$$u'_{\mathrm{p}} - |u_{\mathrm{g}}|_{\mathrm{ref}} l_{\mathrm{n}}\left[\frac{u'_{\mathrm{p}}}{|u_{\mathrm{g}}|_{\mathrm{ref}}} + 1\right] = \frac{f}{t_{\mathrm{p}}}(y_{\mathrm{n}} - y_{\mathrm{p}}) \tag{16}$$

y_{p} is the distance of the point p close to the wall surface.

The particle wall momentum exchange force is given by Tu and Fletcher (1996) as follows:

$$F^{\mathrm{N}}_{\mathrm{wm}} = -C_{\mathrm{N}}\left[1 + \left(\bar{\mathrm{e}}^{\mathrm{N}}_{\mathrm{p}}\right)^2\right]\alpha\rho_{\mathrm{p}}\left|W^{\mathrm{N}}_{\mathrm{p,n}}\right|W^{\mathrm{N}}_{\mathrm{p,n}}(B^{\mathrm{N}})^2 A_{\mathrm{N}} \tag{17}$$

in the direction normal to the surface and

$$F^{\mathrm{T}}_{\mathrm{wm}} = -C_{\mathrm{T}}\left[1 - \left(\bar{\mathrm{e}}^{\mathrm{T}}_{\mathrm{p}}\right)^2\right]\alpha\rho_{\mathrm{p}}\left|W^{\mathrm{T}}_{\mathrm{p,n}}\right|W^{\mathrm{T}}_{\mathrm{p,n}}(B^{\mathrm{T}})^2 A_{\mathrm{N}} \tag{18}$$

in the tangential direction, respectively. $W^{\mathrm{N}}_{\mathrm{p,n}}$ and $W^{\mathrm{T}}_{\mathrm{p,n}}$ are the normal and tangential mean velocities of the particulate phase. A_{N} denotes a face area of the control volume coincident with wall. B_{N} and B_{T} are constants related to the restitution coefficients, which are provided by Tu and Fletcher (1995).

$$B^{\mathrm{N}} = \left\{ \frac{\bar{\mathrm{e}}_{\mathrm{p}}^{\mathrm{N}} \left[1.0 + \left(-\bar{\mathrm{e}}_{\mathrm{p}}^{\mathrm{N}} \right)^{q} \right]}{1.0 + \bar{\mathrm{e}}_{\mathrm{p}}^{\mathrm{N}}} \right\}^{\frac{1}{q+1}} \quad \text{and}$$

$$B^{\mathrm{T}} = \left\{ \frac{\bar{\mathrm{e}}_{\mathrm{p}}^{\mathrm{N}} \left[1.0 + \left(-\bar{\mathrm{e}}_{\mathrm{p}}^{\mathrm{T}} \right)^{q+1} \right]}{1.0 + \bar{\mathrm{e}}_{\mathrm{p}}^{\mathrm{N}}} \right\}^{\frac{1}{q+1}} \tag{19}$$

where q is a factor required for averaging process, $1 \leq q \leq 2$; $q = 1$ refers to momentum average and $q = 2$ corresponds to an energy average. $\bar{\mathrm{e}}_{\mathrm{p}}^{\mathrm{N}}$ and $\bar{\mathrm{e}}_{\mathrm{p}}^{\mathrm{T}}$ are normal and tangential components of restitution coefficient. C_{N} and C_{T} are coefficients of which C_{N} is given by

$$C_{\mathrm{N}} = C_{\lambda} \frac{W_{\mathrm{p,n}}^{\mathrm{N}}}{\left[\sum_{i=1}^{3} (u_{\mathrm{p,n}})^2 \right]^{\frac{1}{2}}} \tag{20}$$

The coefficient C_{λ} is 0.9 according to Tu and Fletcher (1995). C_{λ} has been defined by Tu *et al.* (1996) as:

$$C_{\lambda} = \left(1 - \frac{Y_{\mathrm{p}}}{Y_{\mathrm{N}}} \right)^{\lambda}$$

where $\lambda = -1.3$. λ is an empirical constant. Y_{p} is the normalised distance normal to the wall and is always less than Y_{N}, the normalised particle wall rebounding distance. The coefficient C_{T} is related to the tangential wall momentum exchange force and is modelled as:

$$C_{\mathrm{T}} = \frac{C_{\mathrm{N}}}{y+} \quad \text{for} \quad y+ \leq 11.63 \quad C_{\mathrm{T}} = \frac{C_{\mathrm{N}} \bar{k}}{\ln(Ey+)} \quad \text{for} \quad y+ > 11.63 \tag{21}$$

where $\bar{k}$ and E are the same as in turbulence model of gas phase and $y+>$ has a similar definition but for the particulate flow.

The following section deals with k_{p} and k_{gp} transport equation by consideration of interparticle collision effects. The values of empirical constants for the gas phase turbulence are considered as in conventional single phase flow modelling. These empirical constants are as follows:

$$C_{\mu} = 0.09, \quad C_1 = 1.44, \quad C_2 = 1.92, \quad \sigma_{\kappa} = 1.0, \quad \sigma_{\varepsilon} = 1.3$$

Modelling particle turbulent kinetic energy and fluid particle covariance by consideration of interparticle collision effect

The following section considers formulation for the transport equations relating to the particulate fluctuating motion based on the approach of He and Simonin (1993, 1996). The turbulent momentum transfer between fluctuating motions is obtained in terms of the fluid particle velocity covariance given by an additional transport equation. According to the experimental results and numerical simulations, the interparticle collisions are found to have a significant influence on the coarse particle transport properties in gas-solid turbulent flows even for dispersed phase volumetric fraction $\alpha < 0.01$. The interparticle collision model is developed in the frame of the kinetic theory of diluted gases and the boundary conditions are derived from local study of particle/wall collisions. In addition, the detailed modelling of interparticle collision rate is needed for accurate prediction of coalescence process in dilute two-phase flows. In the kinetic theory of dilute gases, the statistics of binary collisions are derived by assuming that the velocities and positions of any two particles are completely independent. This is the assumption of molecular chaos. In gas-solid flow, however, the probable position and velocities of the two colliding particles will be correlated through their interaction with the surrounding fluid. The present mathematical modelling is based on separate transport equations for the components of the particulate kinetic stress tensor which accounts simultaneously for the turbulent transport mechanism, the dragging along the fluid turbulence and the interparticle collisions. The closure model for the fluid particle velocity correlations is derived by using an approximate Langevin equation (Simonin, 1996) governing the turbulent fluid velocity encountered along discrete particle path. The covariance tensor components are computed with the help of the eddy viscosity concept.

Interparticle collision model

Random collision velocity model. The closure of the interparticle collision terms in the transport equations of the velocity moments presumes the form of the particle-particle pair distribution function f_{22}. In the frame of the kinetic theory of dilute gases, the pair distribution function is written in terms of the single distribution function assuming that the colliding particle velocities are completely independent (molecular chaos assumption) so that:

$$f_{22}(C_{\mathrm{p1}}, C_{\mathrm{p2}}) = f_2(C_{\mathrm{p1}}) f_2(C_{\mathrm{p2}}) \tag{22}$$

The above assumption is theoretically valid only when the relaxation time is much more than the eddy-particle interaction time. However, when the particle relaxation time is of the same order (or smaller) than the eddy-particle interaction time the approaching velocities become correlated through dragging along fluid turbulence. Hence, the correlated collision velocity model has been developed by (Simonin, 1996) accounting for the velocity correlation between the neighbouring particles through a presumed fluid particle joint distribution function.

BGK closure model. Considering dilute dispersed two-phase flows with perfectly elastic particles, it is proposed to use in first approximation the Bhatnagar, Gross and Krook model from the kinetic theory of gases presented by (Simonin, 1996).

$$\left[\frac{\delta f_2}{\delta t}\right] \mathrm{col}\,1 = \frac{-\beta_\mathrm{c}}{\tau_\mathrm{p}^\mathrm{c}}\left[f_2 - f_2^0\right] \tag{23}$$

where $\tau_\mathrm{p}^\mathrm{c}$ is the particle-particle collision time (β_c is constant) and f_2^0 is the equilibrium particle velocity pdf (Maxwellian distribution).

Using the above equation, the collision term appearing in the mean balance equations is given by:

$$C(m_\mathrm{p} u''_{\mathrm{p},i} u''_{\mathrm{p},j}) = -\alpha\rho_\mathrm{p}\frac{\beta_\mathrm{c}}{\tau_\mathrm{p}^\mathrm{c}}\left[\langle u''_{\mathrm{p},i} u''_{\mathrm{p},j}\rangle_\mathrm{p} - \frac{2}{3}k_\mathrm{p}\delta_{ij}\right] \tag{24}$$

The collision term in the kinetic stress transport equation is written as a return-to-isotropy term. Collisions lead to a destruction of the off-diagonal correlations and redistribution of energy among various normal stresses,

$$C(m_\mathrm{p} u''_{\mathrm{p},i} u''_{\mathrm{p},i}) = 0 \tag{25}$$

Third-order moment expansion (Grad's theory). The distribution function in the collision term may be approximated by its third-order expansion in Hermite Polynomials following Grad's theory of rarefied gases presented by (Simonin, 1996).

$$f_2(c_\mathrm{p}, x, t) = \left[1 + \frac{a_{\mathrm{p},ij}}{2T_2^2}\zeta_{\mathrm{p},i}\zeta_{\mathrm{p},j} + \frac{a_{\mathrm{p},ij\mathrm{m}}}{6T_2^3}\zeta_{\mathrm{p},i}\zeta_{\mathrm{p},j}\zeta_{\mathrm{p,m}} - \frac{a_{\mathrm{p},i\mathrm{mm}}}{2T_2^2}\zeta_{\mathrm{p},i}\right] f_2^0(c_\mathrm{p}; x, t) \tag{26}$$

$$\zeta_\mathrm{p} = C_\mathrm{p} - U_\mathrm{p}$$

$$T_2 = \frac{2}{3}k_\mathrm{p},\, a_{\mathrm{p},ij} = \langle u''_{\mathrm{p},i} u''_{\mathrm{p},j}\rangle p - \frac{2}{3}k_\mathrm{p}\delta_{ij}$$

$$a_{\mathrm{p},ij\mathrm{m}} = \langle u''_{\mathrm{p},i} u''_{\mathrm{p},j} u''_{\mathrm{p,m}}\rangle_\mathrm{p}$$

According to the above "hard sphere" collision model, the collisional term in the mean balance equation becomes,

$$C(m_p u''_{p,i} u''_{p,j}) = -\alpha\rho_p \frac{\sigma_c}{\tau_p^c}\left[\langle u''_{p,i} u''_{p,j}\rangle p - \frac{2}{3}k_p\delta_{ij}\right] - \alpha\rho_p \frac{5}{3}\frac{[1-e_c]\sigma_c}{[3-e_c]\tau_p^c}\frac{2}{3}k_p\delta_{ij} \quad (27)$$

with

$$\sigma_c = \frac{[1+e_c][3-e_c]}{5}$$

Hence, the extension to inelastic particles leads to introduce a linear dissipation rate in the kinetic stress transport equations proportional to the collision frequency and function of the restitution coefficient.

The particulate fluctuating motion

The derivation for the closure of dispersed phase fluctuating motion leads to certain particle time scales and the particle relaxation time is defined as:

$$\tau_{fp}^F = F_D^{-1}\frac{\rho_p}{\rho} \quad (28)$$

where the average drag coefficient F_D written in terms of local mean particle Reynolds number is the time scale related to the fluid Lagrangian correlation function computed along particle paths and is mainly affected by the crossing trajectory effect.

$$\tau'_{fp} = \tau'_1\left[1 + C_\beta\xi_r^2\right]^{-1}, \quad \xi_r = |V_r|/\sqrt{\frac{2}{3}k} \quad (29)$$

where C_β has a value of 1.8 in orthogonal directions and 0.45 in the direction of mean relative velocity; V_r is the local relative velocity between the particle and the surrounding fluid; t'_1 is the fluid Lagrangian turbulent time scale and τ_p^c is the interparticle collision time in the frame of kinetic theory and is given by

$$\tau_p^c = \left[\alpha\frac{6}{d_p}\sqrt{\frac{16}{\pi}\frac{2}{3}k_p}\right]^{-1} \quad (30)$$

Particle-phase kinetic stress transport equation

The exchange of momentum due to particle collision remains negligible for $\alpha < 0.1$ and the random motion of the particles provides the principal mechanism for macroscopic transport of momentum and kinetic energy. According to Grad (1949), the influence of the interparticle collisions for monosized elastic hard spheres reduces to a return to isotropy contribution in the dispersed phase kinetic stress equations so that:

$$\alpha\rho_{\mathrm{p}}\left[u_{\mathrm{p,m}}\frac{\delta}{\delta x_{\mathrm{m}}}\right]\langle u''_{\mathrm{p},i}u''_{\mathrm{p},j}\rangle_{\mathrm{p}} = -\frac{\delta}{\delta x_{\mathrm{m}}}\alpha\rho_{\mathrm{p}}\langle u''_{\mathrm{p},i}u''_{\mathrm{p},j}u''_{\mathrm{p,m}}\rangle_{\mathrm{p}}$$

$$-\alpha\rho_{\mathrm{p}}\left[\langle u''_{\mathrm{p},i}u''_{\mathrm{p,m}}\rangle_{\mathrm{p}}\frac{\delta u_{\mathrm{p},j}}{\delta x_{\mathrm{m}}} + \langle u''_{\mathrm{p},j}u''_{\mathrm{p,m}}\rangle_{\mathrm{p}}\frac{\delta u_{\mathrm{p},j}}{\delta x_{\mathrm{m}}}\right] \tag{31}$$

$$-\alpha\rho_{\mathrm{p}}\frac{\sigma_{\mathrm{c}}}{\tau_{\mathrm{p}}^{\mathrm{c}}}\left[\langle u''_{\mathrm{p},i}u''_{\mathrm{p},j}\rangle_{\mathrm{p}} - \frac{2}{3}k_{\mathrm{p}}\delta_{ij}\right] - \alpha\rho_{\mathrm{p}}\frac{2}{\tau_{f\mathrm{p}}^{\mathrm{F}}}\left[\langle u''_{\mathrm{p},i}u''_{\mathrm{p},j}\rangle_{\mathrm{p}} - R_{f\mathrm{p},ij}\right]$$

The subscript p stands for the particle phase. The first term on the right hand side represents the transport of kinetic stress by particle velocity fluctuations and is approximated using an eddy diffusivity closure assumption derived from the third moment equations by neglecting convective transport and mean gradient effects:

$$\frac{\delta}{\delta x_{\mathrm{m}}}\alpha\rho_{\mathrm{p}}\langle u''_{\mathrm{p},i}u''_{\mathrm{p},j}u''_{\mathrm{p,m}}\rangle_{\mathrm{p}} = -\frac{\delta}{\delta x_{\mathrm{m}}}\left[\alpha\rho_{\mathrm{p}}k'_{\mathrm{p,mn}}\frac{\delta}{\delta x_{\mathrm{n}}}\langle u''_{\mathrm{p},i}u''_{\mathrm{p},j}\rangle_{\mathrm{p}}\right]$$

where the kinetic stress diffusivity tensor is written as

$$k'_{\mathrm{p,mn}} = \left[\frac{\tau'_{\mathrm{fp}}}{\xi'_{\mathrm{fp}}}R_{\mathrm{fp,mn}} + \frac{\tau^{\mathrm{F}}_{\mathrm{fp}}}{\xi^{\mathrm{F}}_{\mathrm{fp}}}\langle u''_{\mathrm{p,m}}u''_{\mathrm{p,n}}\rangle_{\mathrm{p}}\right]\left[1 + \frac{\tau^{\mathrm{F}}_{\mathrm{fp}}}{\xi^{\mathrm{F}}_{\mathrm{fp}}}\frac{\xi_{\mathrm{c}}}{\tau^{\mathrm{c}}_{\mathrm{p}}}\right]^{-1}$$

where

$$\xi^{\mathrm{F}}_{\mathrm{fp}} = \frac{9}{5}, \quad \xi_{\mathrm{c}} = \frac{8}{25}, \quad \xi'_{\mathrm{fp}} = \frac{3}{2}\frac{C_\mu}{C_S}, \quad C_S = 0.25$$

The second term represents the production by the mean particle velocity gradient.

The third term accounts for the interparticle collision in the frame of Grad's theory ($\sigma_{\mathrm{c}} = 0.8$), this complementary term leads to destruction of the off-diagonal correlations and redistribution of energy among the various diagonal components of the kinetic stress tensor.

The last term represents the interaction with fluid turbulent motion, and the fluid particle symmetric correlation tensor $R_{\mathrm{fp},ij}$ is given by:

$$R_{\mathrm{fp},ij} = \frac{1}{2}\left[\langle u''_{\mathrm{f},i}u''_{\mathrm{p},j}\rangle_{\mathrm{p}} + \langle u''_{\mathrm{p},i}u''_{\mathrm{f},j}\rangle_{\mathrm{p}}\right]$$

The subscripts f and p refers to the fluid particle and phase, respectively.

The extension of Grad's theory to inelastic particles leads to a complementary dissipative term in the kinetic stress transport equation (31):

$$-\alpha\rho_{\mathrm{p}}\varepsilon_{\mathrm{c},ij} = -\alpha\rho_{\mathrm{p}}\frac{1}{3}\left[\frac{1-\mathrm{e}_{\mathrm{c}}^{2}}{\tau_{\mathrm{p}}^{\mathrm{c}}}\right]\frac{2}{3}k_{\mathrm{p}}\delta_{ij}$$

where $\mathrm{e_c}$ is the restitution coefficient of inter particle collisions.

The given parameters of the return to isotropy term and kinetic stress diffusivity tensor adopt the general forms

$$\sigma_{\mathrm{c}} = \frac{(1+\mathrm{e_c})(3-\mathrm{e_c})}{5} \quad \xi_{\mathrm{c}} = \frac{(1+\mathrm{e_c})(49-33\mathrm{e_c})}{100} \tag{32}$$

For perfectly elastic particles ($\mathrm{e_c} = 1$), the Grad values are $\sigma_{\mathrm{c}} = 4/5$ and $\xi_{\mathrm{c}} = 8/25$ for perfectly elastic particles.

Turbulent kinetic energy transport model

The two equation turbulence models viz. k_{p}-k_{gp} based on eddy viscosity assumption is derived from separate particle kinetic stress equation. The kinetic stress tensor components are computed with the eddy viscosity concept,

$$\rho_{\mathrm{p}}\langle u''_{\mathrm{p},i}u''_{\mathrm{p},j}\rangle_{\mathrm{p}} = -\rho_{\mathrm{p}}\varepsilon_{\mathrm{p}}\left[\frac{\delta u_{\mathrm{p},i}}{\delta x_j}+\frac{\delta u_{\mathrm{p},j}}{\delta x_i}\right]+\frac{2}{3}\delta_{ij}\left[\rho_{\mathrm{p}}k_{\mathrm{p}}+\rho_{\mathrm{p}}\varepsilon_{\mathrm{p}}\frac{\delta u_{\mathrm{p,m}}}{\delta x_{\mathrm{m}}}\right] \tag{33}$$

The expression for eddy-viscosity of particle phase is obtained from off-diagonal correlation equation (31) considering that the fluid and particle mean velocity gradients are almost equal.

$$\varepsilon_{\mathrm{p}} = \left[\varepsilon'_{\mathrm{fp}}+\frac{1}{2}\tau^{\mathrm{F}}_{\mathrm{fp}}\frac{2}{3}k_{\mathrm{p}}\right]\left[1+\frac{\tau^{\mathrm{F}}_{\mathrm{fp}}}{2}\frac{\sigma_{\mathrm{c}}}{\tau^{\mathrm{c}}_{\mathrm{p}}}\right]^{-1} \tag{34}$$

The expression for fluid turbulent viscosity is given as:

$$\varepsilon'_{\mathrm{fp}} = \frac{1}{3}k_{\mathrm{gp}}\tau'_{\mathrm{fp}} \quad \text{where} \quad k_{\mathrm{gp}} = \langle u''_{\mathrm{f},i}u''_{\mathrm{p},j}\rangle_{\mathrm{p}}$$

The eddy diffusivity coefficient is written as:

$$K'_{\mathrm{p}} = \left[\frac{\varepsilon'_{\mathrm{fp}}}{\sigma_{\mathrm{q}}}+\frac{5}{9}\tau^{\mathrm{F}}_{\mathrm{fp}}\frac{2}{3}k_{\mathrm{p}}\right]\left[1+\frac{5}{9}\tau^{\mathrm{F}}_{\mathrm{fp}}\frac{\xi_{\mathrm{c}}}{\tau^{\mathrm{c}}_{\mathrm{p}}}\right]^{-1}$$

The dissipation rate due to inelastic collisions is:

$$\varepsilon_{\mathrm{c}} = \frac{1}{2}\frac{\left(1-\mathrm{e}_{\mathrm{c}}^{2}\right)}{\tau^{\mathrm{c}}_{\mathrm{p}}}\frac{2}{3}k_{\mathrm{p}}$$

The interaction term accounting for continuous phase influence becomes

$$\pi_{\mathrm{qp}} = -\alpha\rho_{\mathrm{p}}\frac{1}{\tau_{\mathrm{fp}}^{\mathrm{F}}}(2k_{\mathrm{p}} - k_{\mathrm{gp}})$$

$$\frac{\delta}{\delta x_j}(\alpha\rho_{\mathrm{p}}u_{\mathrm{p}j}k_{\mathrm{p}}) = \frac{\delta}{\delta x_j}\left(\alpha\rho_{\mathrm{p}}\frac{K'_{\mathrm{p}}}{\sigma_{\mathrm{p}}}\frac{\delta k_{\mathrm{p}}}{\delta x_j}\right) + P_{\mathrm{kp}} - \alpha\rho_{\mathrm{p}}\varepsilon_{\mathrm{c}} + \pi_{\mathrm{qp}} \tag{35}$$

where,

$$P_{\mathrm{kp}} = -\alpha\rho_{\mathrm{p}}\langle u''_{\mathrm{p},i}u''_{\mathrm{p},j}\rangle_{\mathrm{p}}\frac{\delta u_{\mathrm{p},i}}{\delta x_j}.$$

In case the interparticle collision effect is neglected, the term $\alpha\rho_{\mathrm{p}}\varepsilon_{\mathrm{c}}$ in equation (35) will be come zero.

Fluid particle covariance equation

The covariance components are computed by resorting to the eddy viscosity concept. The subscripts f and p refers to the fluid and particle phases.

$$\rho_{\mathrm{p}}\langle u''_{\mathrm{f},i}u''_{\mathrm{p},j}\rangle_{\mathrm{p}} = -\rho_{\mathrm{p}}\varepsilon'_{\mathrm{fp}}\left(\frac{\delta u_{\mathrm{f},j}}{\delta x_j} + \frac{\delta u_{\mathrm{p},j}}{\delta x_i}\right) + \frac{1}{3}\delta_{ij}\left[\rho_{\mathrm{p}}k_{\mathrm{gp}} + \rho_{\mathrm{p}}\varepsilon'_{\mathrm{fp}}\left(\frac{\delta u_{\mathrm{f,m}}}{\delta x_{\mathrm{m}}} + \frac{\delta u_{\mathrm{p,m}}}{\delta x_{\mathrm{m}}}\right)\right] \tag{36}$$

The fluid turbulent viscosity is written in terms of the fluid particle velocity covariance k_{gp} and eddy particle interaction time τ'_{fp} :

$$\varepsilon'_{\mathrm{fp}} = \frac{1}{3}k_{\mathrm{gp}}\tau'_{\mathrm{fp}} \quad \text{where} \quad k_{\mathrm{gp}} = \langle u''_{\mathrm{f},i}u''_{\mathrm{p},j}\rangle_{\mathrm{p}}$$

The fluid particle covariance transport equation is therefore, formulated as:

$$\frac{\delta}{\delta x_j}(\alpha\rho_{\mathrm{p}}u_{\mathrm{p}j}k_{\mathrm{gp}}) = \frac{\delta}{\delta x_j}\left(\alpha\rho_{\mathrm{p}}\frac{\varepsilon'_{\mathrm{fp}}}{\sigma_{\mathrm{q}}}\frac{\delta k_{\mathrm{gp}}}{\delta x_j}\right) - \alpha\rho_{\mathrm{p}}\varepsilon_{\mathrm{fp}} + \pi_{\mathrm{qfp}} + Pk_{\mathrm{gp}} \tag{37}$$

The first term on the right hand side represents the transport of covariance by velocity fluctuations.

The second term models the destruction rate due to viscous action in fluid phase and loss of correlation by crossing-trajectories effects.

$$\varepsilon_{\mathrm{fp}} = k_{\mathrm{gp}}/\tau'_{\mathrm{fp}}$$

The third term represents interphase turbulent momentum transfer.

$$\pi_{\mathrm{qfp}} = -\alpha\rho_{\mathrm{p}}\frac{1}{\tau_{\mathrm{fp}}^{\mathrm{F}}}[(1 + X_{\mathrm{fp}})k_{\mathrm{gp}} - 2k - 2X_{\mathrm{fp}}k_{\mathrm{p}}]$$

where,

$$X_{\mathrm{fp}} = \frac{\alpha\rho_{\mathrm{p}}}{\beta\rho}$$

The last term represents production by mean velocity gradients.

$$Pk_{\mathrm{gp}} = -\alpha\rho_{\mathrm{p}}\langle u''_{\mathrm{f},i}u''_{\mathrm{p},j}\rangle_{\mathrm{p}}\frac{\delta u_{\mathrm{p},i}}{\delta x_j} - \alpha\rho_{\mathrm{p}}\langle u''_{\mathrm{p},i}u''_{\mathrm{f},j}\rangle_{\mathrm{p}}\frac{\delta u_{\mathrm{f},i}}{\delta x_j}$$

The fluid particle velocity covariance equation may retain the form given in equation (11) as shown below:

$$\frac{\delta}{\delta x_j}\{\alpha\rho_{\mathrm{p}}(u_j + u_{\mathrm{p}j})k_{\mathrm{gp}}\} = \frac{\delta}{\delta x_j}\left\{\alpha\rho_{\mathrm{p}}\left(\frac{\varepsilon_{\mathrm{f}}}{\sigma_{\mathrm{f}}} + \frac{\varepsilon_{\mathrm{p}}}{\sigma_{\mathrm{p}}}\right)\frac{\delta k_{\mathrm{gp}}}{\delta x_j}\right\} + P_{\mathrm{kgp}} - \alpha\rho_{\mathrm{p}}\varepsilon_{\mathrm{fp}} - \pi_{\mathrm{gp}}$$

In the above equation the terms P_{kgp} and π_{gp} have already been defined in equation (11). The third term on the right hand side models the destruction rate due to viscous action in fluid phase as defined in equation (37). The particle eddy viscosity ε_{p} in the above equation is defined in equation (34).

Algebraic relation for particle phase eddy viscosity

An algebraic relation relating particle phase eddy viscosity in terms of fluid phase eddy viscosity is proposed by Choi and Chung (1983) and Zhou *et al.* (1994):

$$\varepsilon_{\mathrm{p}} = \frac{\varepsilon_{\mathrm{f}}}{\left\{1 + \left(\frac{t^*}{t_{\mathrm{L}}}\right)^2\right\}} \tag{38}$$

where t is the particle relaxation time given by $t^* = \rho_{\mathrm{p}}d_{\mathrm{p}}^2/18\mu$ and t_{L} is the Lagrangian integral time scale.

Boundary conditions and computational details

For the computation of two phase flows the boundary conditions usually prescribed are:

Inlet : $u, v, w, u_{\mathrm{p}}, v_{\mathrm{p}}, w_{\mathrm{p}}, p, \bar{P}, \alpha$ are prescribed and are assumed uniform.

wall : $u = v = w = v_{\mathrm{p}} = k = k_{\mathrm{p}} = k_{\mathrm{gp}} = 0$

The Eulerian wall boundary conditions are set for the axial and tangential particle velocity through particle-wall collision model.

Symmetry axis:

$$\frac{\delta u}{\delta y} = \frac{\delta u_{\mathrm{p}}}{\delta y} = \frac{\delta w}{\delta y} = \frac{\delta w_{\mathrm{p}}}{\delta y} = \frac{\delta k}{\delta y} = \frac{\delta \varepsilon}{\delta y} = \frac{\delta k_{\mathrm{p}}}{\delta y} = \frac{\delta k_{\mathrm{gp}}}{\delta y}$$

$$v = 0, \quad v_{\mathrm{p}} = 0$$

where u, v, w are fluid velocities in the x, y and z (longitudinal) directions, and subscript p stands for particle.

The computational grid chosen was (15×15), i.e. 225 points on the cross stream plane. The grid size was increased to (20×20), i.e. 400 points on the cross stream plane and variation in computational results was minimal. Hence, the (15×15) grid was considered as optimum from the point of view of numerical convergence, reliability of predictions and economical computer storage. The numerical solutions depicted good convergence after a prescribed number of iterations and percentage error in continuity equation was less than 0.01. The step size considered was reasonably small and the solution provided a fully developed flow profile at about 500 forward steps, i.e. grid points in the marching direction for straight ducts. For curved ducts, representative predicted particle concentration profile was obtained at 200 forward steps, i.e. grid points in the streamwise direction.

Solution procedure

The governing equations are solved by Parabolic procedure outlined by Patankar *et al.* (1975). All the variables are stored two dimensionally and a Tri-Diagonal Matrix Algorithm is adopted with upwind finite differencing scheme, after discretization of governing equations by control volume integration. The staggered grid system has been utilised, i.e. the grid system for u, u_{p} and v, v_{p} velocity components are staggered from the main control volume. The solution method is outlined below.

(1) The average pressure $\bar{p}$ and the pressure distribution $p\ (x, y)$ at the downstream section are assigned guessed values.

(2) The three-dimensional equations of momentum for fluid phase are solved to obtain a first approximation to the downstream velocity distribution.

(3) The mean pressure $\bar{p}$ and the axial velocities are thereupon corrected with reference to continuity and linearised longitudinal momentum equation so as to ensure that the mass flow rate through the downstream section is the same as through the upstream section.

(4) Since the cross-stream velocities do not satisfy the continuity equation locally, a Poisson' equation is derived from this equation and the two linearised momentum equation; the Poisson equation is then solved for correction of the pressure (p) field. The cross-stream velocities are then corrected accordingly.

(5) The steps (i)-(iv) are repeated iteratively till equation of continuity is satisfied. The k and ε equations are then solved to obtain new distribution of viscosity.
(6) The separate transport equations for k_{p} and k_{gp} are solved to generate the particle phase eddy viscosity.
(7) The three dimensional equations of momentum for particle phase are solved to obtain particle velocity field.
(8) The particle concentration distribution is determined from the equation of continuity for the particle phase.
(9) A new downstream station is chosen and steps (i)-(viii) are repeated.

Disussion on numerical predictions

Numerical predictions in straight conduits

Figures 1 and 2 show computed air and particle velocity profiles in a straight vertical pipe for the situation ($d_{\mathrm{p}} = 406\,\mu\mathrm{m}$, $\rho_{\mathrm{p}}/\rho = 860$, $\mathrm{Re} = 4.27 \times 10^4$) and particle volumetric fractions of 1×10^{-3} and 5.14×10^{-3}, respectively. The particulate phase velocity profile shows a relatively flatter nature in both those cases. The air velocity profile shows a more pronounced flatness with increased particle concentration. It is evident from the figures that the velocity of the dispersed phase is somewhat higher than that of air in the wall region as the air flow is subjected to no-slip condition at the wall while the dispersed phase slips by. The velocity of the particle is, however, smaller than the air velocity over most of the cross section. The dispersed phase acts as a source of momentum for the air at near wall region and the air velocity experiences deceleration in the core region to satisfy mass conservation. The deceleration is caused by particle drag which results in flattening of the air velocity profile in the core region. The figures depict that the location at which the slip velocity vanishes is shifted away from the wall as the particle mass loading ratio is decreased.

The figures also compare present predictions with the experimental data of Tanaka *et al.* presented by He and Simonin (1993). There is a good agreement between predictions and experimental data for the dispersed phase velocity profile. Comparison is depicted between predictions based on k_{p} and k_{gp} equations (10) and (11) and that obtained through k_{p} and k_{gp} equations (35) and (37). These computations are in turn compared with that obtained through eddy viscosity determined by equation (38). These comparisons show closeness in agreement. However, agreement between predictions and experimental data is closer with the k-ε-k_{p} models than using the algebraic relation for particle phase eddy viscosity.

Numerical predictions on particle concentration in curved ducts

The curved duct under consideration is a pipe bend approximating a square section. The erosion caused by particle impingement for this non-circular

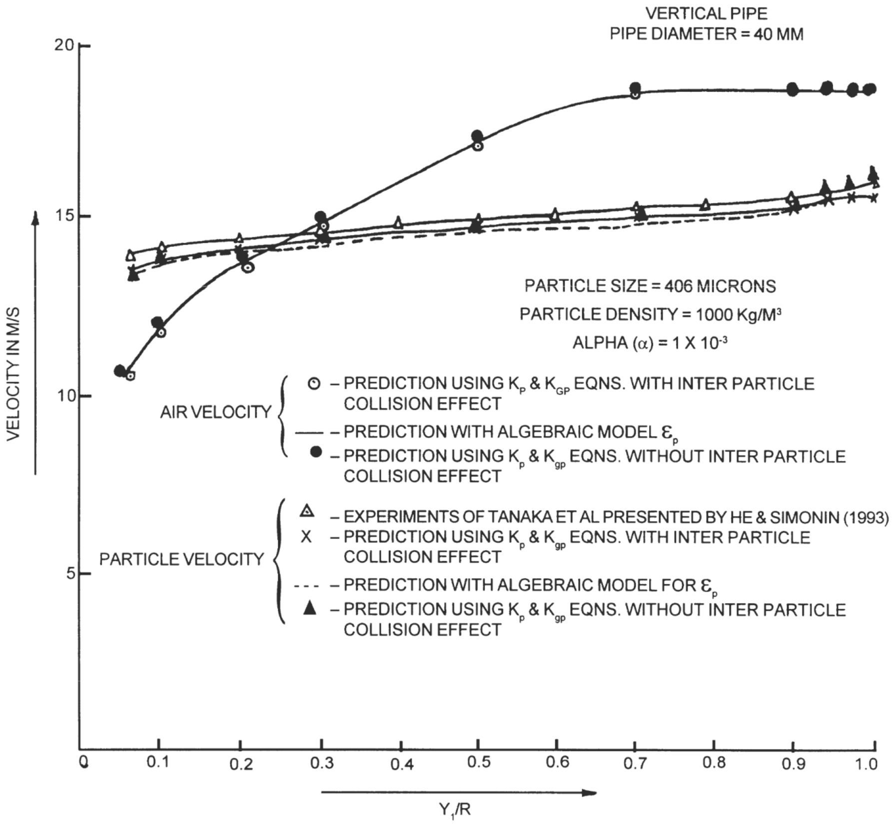

Figure 1.
Velocity distribution for two phase flow in straight vertical pipe: comparison between predictions and experiment

type bend is reduced substantially owing to uniformity in particle concentration distribution along the outer wall in the Y-direction as shown by Mitter (2000) and Mitter *et al.* (1993) through predictions. The coal pipe bends of circular section had undergone serious erosion owing to localised particle concentration as shown by Mitter (2000) and Mitter *et al.* (1998). Figure 3 shows the predicted particle concentration profile between the inner and outer walls of the curved circular pipe through the present modified Eulerian approach. This figure depicts the zonalysed particle concentration at the outer wall. Comparison is shown between the predictions obtained through k_{p} and k_{gp} equations (10) and (11) and that determined through k_{p} and k_{gp} equations (35) and (37). The comparison shows a very close agreement (Mitter, 2000). The particle mass loading ratio m considered for all computations is 0.45.

For curved ducts Dean number is defined as:

$$D_{\mathrm{e}} = \mathrm{Re}\sqrt{\frac{a}{r}}$$

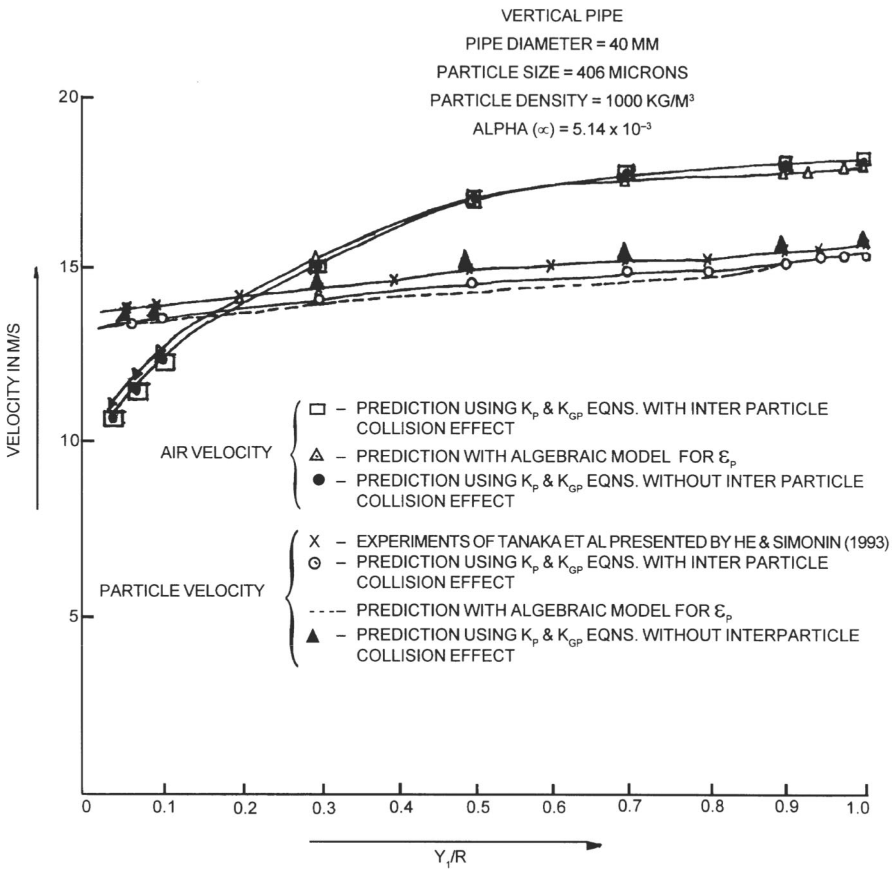

Figure 2.
Velocity profiles for two phase flow in straight vertical pipe: comparison between prediction and experiment

where r is the radius of curvatures, a the radius of the cross section, and Re the Reynolds number.

Effects of Dean number. The numerical predictions are based on k_{p} and k_{gp} equations (35) and (37). Figure 4 shows the computed particle concentration between the inner and outer walls of a curved square duct for Dean number 2.45×10^5, 2.2×10^5, 2.0×10^5 and 1.8×10^5 at a distance of 2.0 m from the inlet. The particle size considered is 100 μm. The figure depicts much higher concentrations towards outer wall than inner wall owing to centrifugal effects as shown by Mitter *et al.* (1993, 1998).

As the Dean number is increased the centrifugal effect is higher and the particles migrate towards the outer wall at a greater rate leading to higher particle concentration near this wall. Hence, the Dean number 1.8×10^5 leads to lowest predicted concentration near outer wall whereas the Dean number

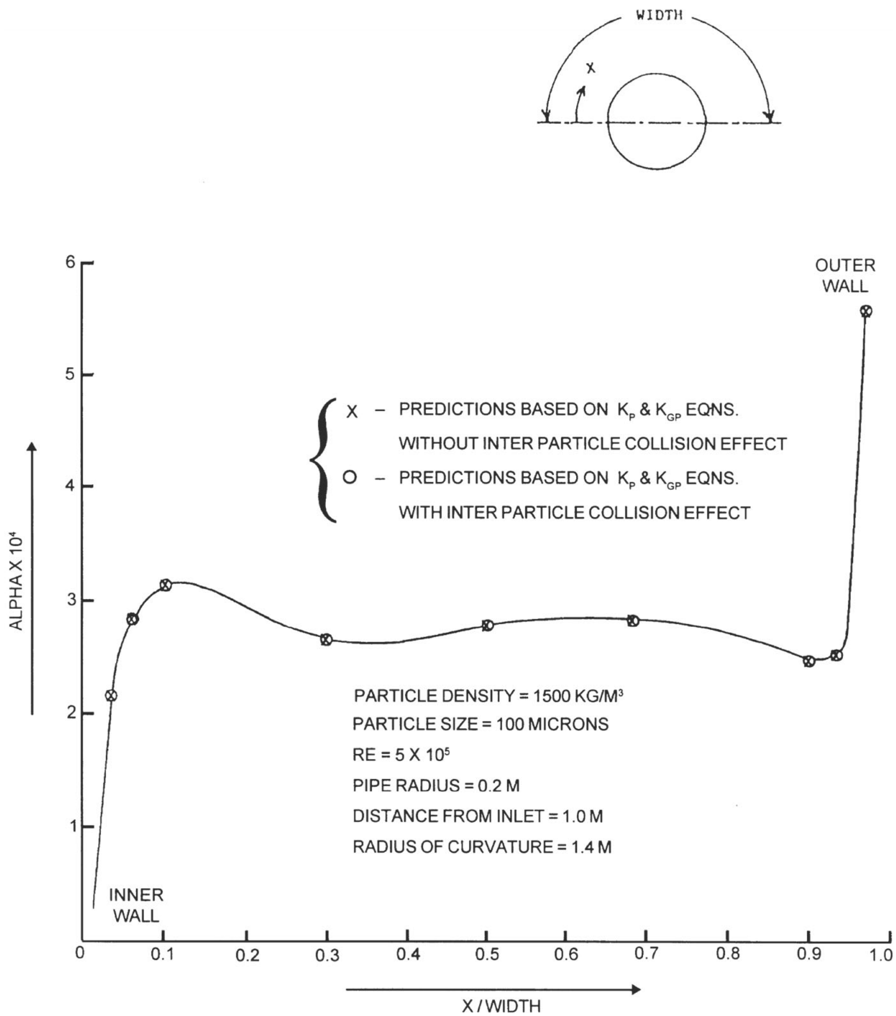

Figure 3.
Particle concentration profile along the circumference between the inner and outer wall of a curved circular pipe

2.45×10^5 results in highest computed particle concentration near this wall. This feature has been depicted by Mitter (2000).

Effects of particle size. The k_p and k_{gp} equations (35) and (37) are utilised for computations. The numerically predicted particle concentration profile between the inner and outer walls of the curved square duct at a distance of 2.0 m from the inlet is shown for different particle sizes, viz. 100, 120, 150, and 200 μm, respectively, in Figure 5. The Dean number considered is 2.2×10^5.

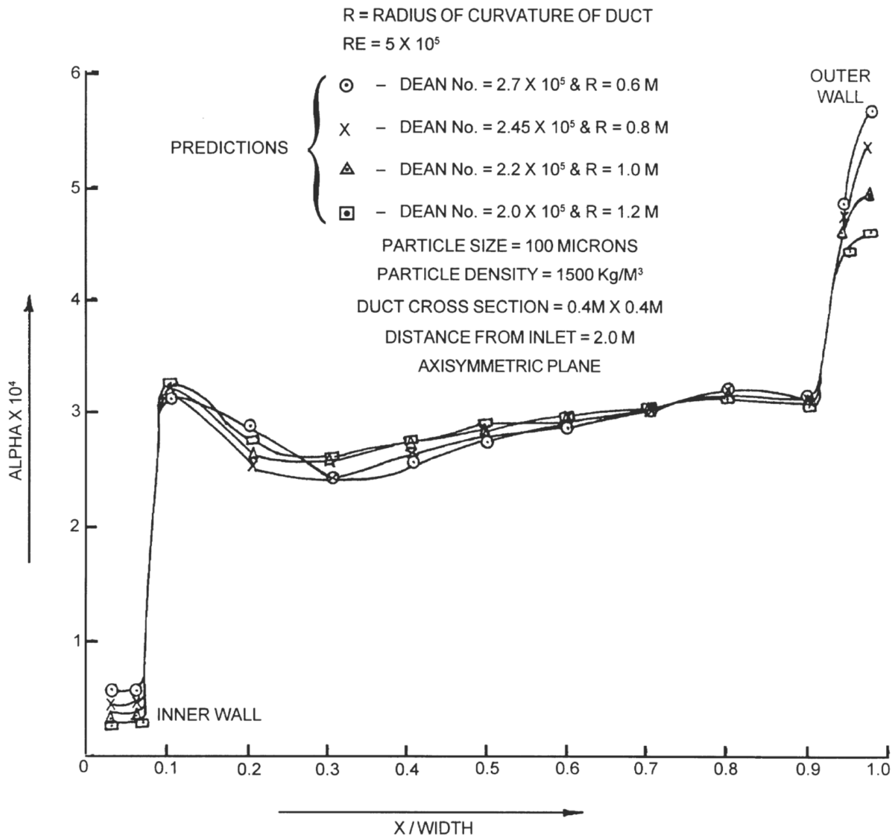

Figure 4.
Particle concentration distribution in curved square duct for different Dean numbers

As depicted by Mitter (2000) and Mitter *et al.* (1998), the acceleration is higher for smaller particles; hence, the migration of these particles towards the outer wall is at a greater rate. The centrifugal force hence has a greater effect when the particle size is reduced. This phenomenon leads to highest concentration near the outer wall for smallest size particle, viz. 100 μm among the four different particle sizes shown in Figure 5.

Experimental research

This section deals with the results and discussions related to the experimental research.

Pressure drop measurement and erosion studies for two phase flow of air coal mixtures

Pressure drop measurements have been conducted in straight vertical and horizontal portions in coal pipes conveying two-phase air coal mixtures to

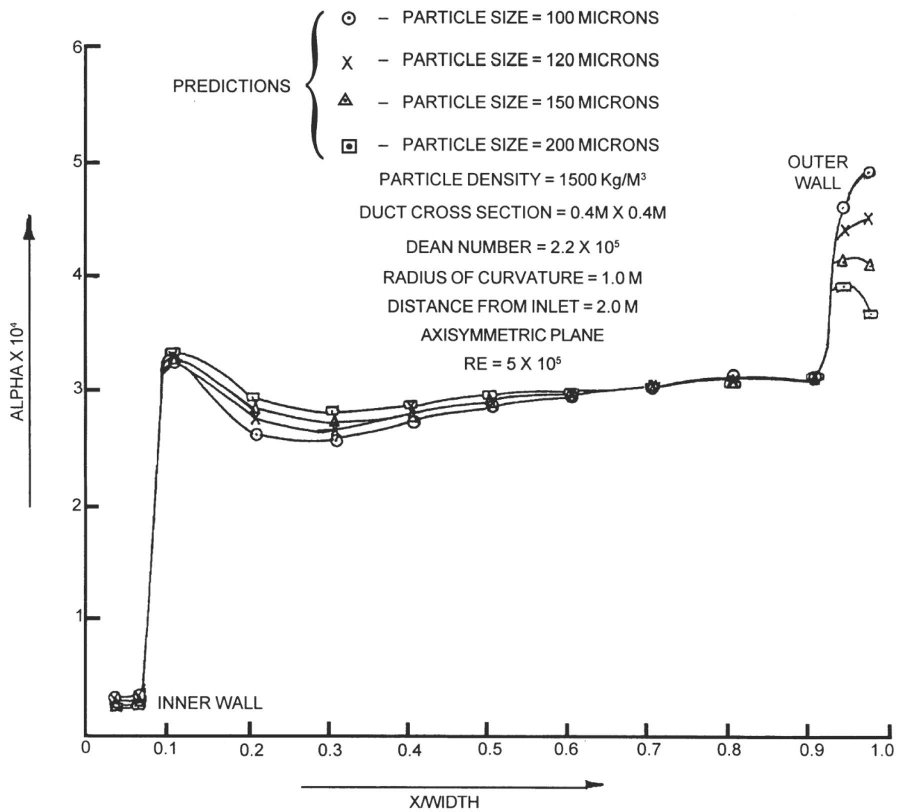

Figure 5.
Particle concentration profile in curved square duct for different particle sizes

burners in a thermal power plant. Similar pressure drop measurements have also been performed in the curved sections of non-circular as well as circular coal pipes. These experimental results are compared with the numerical predictions based on k_p and k_{gp} equations with interparticle collision effects and the comparisons are presented in Table I. It is evident from Table I that the predicted pressure drops for both straight and curved ducts agree well with the experimental data (Mitter, 2000). An uncertainity analysis showed that the uncertainities involved in the pressure drop measurements were within 3 per cent.

For the above duct configuration the circular coal pipe has a diameter of 0.43 m and the square coal pipe bend is of cross section 0.4×0.4 m.

The details of erosion studies for circular and square sectioned coal pipe bends are depicted by Mitter (2000). The square section curved duct has uniform erosion along the inner surface of the outer wall in the Y-direction as well as longitudinal direction. This is physically observed and the erosion is relatively less in this case. The circular curved duct undergoes a substantial

Duct configuration	Distance between pressure tappings (m)	Mass flow rate of air (kg/s)	Pressure drop due to two phase flow of air coal mixture with coal air loading ratio of 0.45 (mm water) Prediction	Experimental
Vertical straight pipe	4.2	4.05	31	27
Horizontal straight pipe	4.8	4.05	32.2	27
Non-circular square curved duct (90° bend)	2.6	4.05	62	65
Circular curved duct (90° bend)	2.85	4.05	61.8	67

Table I.

impingment zonalised erosion (forming cavity) on the outer wall and also the erosion pattern is non-uniform along this wall in the longitudinal direction.

The following is the comparative performance study from erosion point of view of various types of coal pipe bends used on a 210 MW unit of a large thermal power plant, from inception in 1982 to date.

(1) *Year 1982*. Ordinary grey cast iron bend (RC 25 hardness) having circular cross section with internal diameter of 425 mm, having uniform wall thickness of 20 mm. This bend had leak-free life for only 6 months and replacement life of 1 year.

(2) *Year 1986*. Bassalt lined Grey cast iron bend (RC 25 hardness) having circular cross section with cast iron wall thickmess of 15 mm. The bassalt lining had a thickness of 10 mm and possessed RC 50 hardness. The cavity formation by particle impingment was prominent. This bend had leak-free life of 1 year and replacement life of 2 years.

(3) *Year 1993*. Experimental M–4 square sectioned mild steel bend (RC 25 hardness) had a leak-free life of 3 years and replacement life of 4 years.

(4) *Year 1994*. M–4 square sectioned bend with 10 mm. RC 50 liner (total outer wall thickness being 20 mm, i.e. the same as circular pipe bend) had a leak-free life of 5 years and a replacement life of 6 years.

Conclusion

Based on the work it is concluded that Eulerian mathematical models prove effective in simulation of two phase flow fields in confined systems. The computed fluid and particle velocities agreed well with the experimental data. It is observed that there is a close agreement in predictions of mean parameters for two phase flow field by using k_{p} and k_{gp} equations with and without interparticle collision effects.

For curved ducts when Dean number is increased the predicted particle concentration near the outer wall is higher than that at the lower Dean number owing to greater centrifugal effects. As the particle size is increased the computed particle concentration near the outer wall is lower than that for smaller particle size, obviously because of the greater inertia for the larger particles. Hence, the computations predict qualitatively the physical situation in case of curved duct.

Comparison of pressure drop measurements of two-phase flows in straight and curved ducts show good agreement with numerical predictions based on the two fluid model.

The non-circular (square) curved sections of coal pipes conveying two-phase flows are subjected to less erosion owing to uniformity in particle concentration along the outer wall. The circular curved sections are subjected to serious erosion owing to zonalysed particle concentration on the outer wall. This aspect has been established through the numerical predictions and experimental results.

References

Choi, Y.D. and Chung, M.K. (1983), "Analysis of turbulent gas-solid suspension flow in a pipe", *Trans. ASME J. Fluids Eng.*, Vol. 105, pp. 329-34.

Durst, F. and Milojevic, D. (1984), "Eulerian and Lagrangian prediction of particulate two phase flows: a numerical study", *Appl. Math. Model.*, Vol. 8, pp. 101-4.

Gidaspow, D. (1994), *Multiphase flow and Fluidization, Continuum and Kinetic Theory Descriptions*, Academic Press, New York, NY.

He, J. and Simonin, O. (1993), "Non-equilibrium prediction of the particle phase stress tensor in vertical pneumatic conveying", *Gas-Solid Flows*, pp. 253-63, FED-Vol. 166, ASME.

Mitter, A. (2000), "An analytical and experimental study on two phase flow of gas solid suspensions through confined system", PhD dissertation, Indian Institute of Technology, Kharagpur.

Mitter, A., Malhotra, J.P. and Jadeja, H.T. (1998), "Numerical predictions and experimental studies on two phase gas-particle transport phenomenon in confined systems", *Proceedings of International Conference on Theoretical, Applied, Computational and Experimental Mechanics*, I.I.T., Kharagpur.

Mitter, A., Malhotra, J.P., Sreedhar, B.N. and Jadeja, H.T. (1993), "An analytical and experimental study on two phase flow of gas solid suspensions through confined systems", *Journal of Energy Heat Mass Transfer*, Vol. 15, pp. 357-66.

Patankar, S.V., Pratap, V.S. and Spalding, D.B. (1975), "Prediction of turbulent flow in curved pipes", *J. Fluid Mech.*, Vol. 67, pp. 583-93.

Rizk, M.A. and Elghobashi, S.E. (1989), "A two-equation turbulence model for dispersed dilute confined two-phase flows", *Int. J. Multiphase Flow*, Vol. 15, pp. 119-33.

Simonin, O. (1996), *Combustion and Turbulence in Two-phase Flows*, Von Karman Institute for Fluid Dynamics, Lecture Series 1996-02.

Sommerfeld, M. (2001), "Validation of a stochastic Lagrangian modelling approach for inter-particle collisions in homogeneous isotropic turbulence", *Int. J. Multiphase Flow*, Vol. 27 No. 10, pp. 1829-58.

Sommerfeld, M. (2003), "Analysis of collision effects turbulent gas-particle flow in a horizontal channel – part 1: particle transport", *Int. J. Multiphase Flow*, Vol. 29 No. 4, pp. 675-99.

Tsirkunov, Yuri, M., Volkov, Alekgei, N., Tarasova and Natalia, V. (2002), "Full Lagrangian approach to the calculation of dilute dispersed phase flows: advantages and applications", FED, Vol. 257 No. 2A, pp. 409-22, *ASME*.

Tu, J.Y. (1997), "Computation of turbulent two phase flow on overlapped grids", *Numer. Heat Transfer*, Part-B, Vol. 32, pp. 175-95.

Tu, J.Y. and Fletcher, C.A.J. (1994), "An improved model for particulate turbulence modulation in confined two-phase flows", *Int. Commun. Heat Mass Transfer*, Vol. 21 No. 6, pp. 775-88.

Tu, J.Y. and Fletcher, C.A.J. (1995), "Numerical computation of turbulent gas-particle flow in a 90° bend", *AICHE J.*, Vol. 41, pp. 2187-97.

Tu, J.Y. and Fletcher, C.A.J. (1996), "Computational modelling of particle dispersion in a backward-facing step flow", FED-Vol. 236, FED Conference, *ASME*, Vol. 1, pp. 283-9.

Tu, J.Y., Lee, B.E. and Fletcher, C.A.J. (1996), "Eulerian modelling of particle-wall collisions in confined gas-particle flows via a Lagrangian approach", FED-Vol. 236, FED Conference, Vol. 1, pp. 751-8, *ASME*.

Zhang, Y. and Reese, J.M. (2001), "Particle-gas turbulence interactions in a kinetic theory approach to granular flows", *Int. J. Multiphase Flow*, Vol. 27 No. 11, pp. 1945-64.

Zhou, L.X., Liao, C.M. and Chan, T. (1994), "A unified second-order moment two phase model for simulating gas-particle flows", FED-Vol. 185, Numer. Methods Multiphase Flows, pp. 307-13, *ASME*.

Further reading

Lavieville, J., Dentsch, E. and Simonin, O. (1995), "Large eddy simulation of interactions between colliding particles and a homogeneous isotropic turbulence field", FED-Vol. 228, Gas-Solid Flows, ASME.

Soo, S.L. (1967), *Fluid Dynamics of Multiphase Systems*, Blaisdell Publishing Company.